RESEARCH ARTICLE

Editorial Process: Submission:09/01/2025 Acceptance:05/10/2026 Published:05/18/2026

Detection of Stages of Oral Cavity Lesions Using a Fluorescence Portable Device and Their Classification by Artificial Intelligence Tools

Pavan Kumar[1]*, Amar Nath Sah[2], Vikrant Yashwant Ganvir[3], Asima Pradhan[4], Roshni Rathour[5]

Abstract

Objective: In the present study, we utilized a fluorescence-based portable device for the detection of oral lesions, as well as AI tools for the classification of the spectroscopic data. The portable device comprises optical components (lens, filters, and beam splitter), a laser, a spectrometer, and other accessories (laptop, fibers, etc.). Laser light (λ_{exc} = 405 nm), irradiated onto the lateral border of the tongue (LBT) of the oral cavity tissue, excites the fluorophores FAD (λ_{emi} ≈ 500 nm) and Porphyrin (λ_{emi} ≈ 634 nm) more significantly than the others.**Methods:** Fluorescence spectra were recorded from three groups, i.e., OSCC, Dysplastic, and Normal, in the range of 450 to 750 nm. Among these groups, OSCC and Dysplastic patients exhibited a significant rise in porphyrin fluorescence.**Result:** Data analysis was accomplished using AI tools, namely Principal Component Analysis (PCA), K-Nearest Neighbors (KNN), Naïve Bayes, Linear and Quadratic Discriminant Analysis (LDA & QDA), and ROC analysis. Among these AI tools, the PCA-based QDA classifier was capable of discerning among the groups with slightly higher accuracy values (≈ 98%) than the other AI tools. **Conclusion:** Results reveal that the in-house-built fluorescence device, along with QDA, would be an elegant tool for the identification of oral lesions at the preliminary stage.

Keywords: Oral lesions- fluorescence- porphyrin- artificial intelligence tools

Asian Pac J Cancer Prev, **27 (5)**, 1757-1763

Introduction

To detect oral lesions, quite a few conventional methods are utilized by the clinicians. Among them, visual inspection is first step towards it. Apart from it, techniques like brush biopsy, ViziLite, toluidine blue, tissue biopsy etc. were utilized by the clinicians. In these methods, tissue biopsy with the histopathology is the gold standard for the confirmation of various stages (benign, precancerous, OSCC) of oral lesions. Although, histopathology is the utmost reliable method but its invasive and lengthy attributes make it ineffective. Other limitation associated with this method is its inability to find the appropriate area for biopsy. Because of these limitations, patients have to undergo quite a few biopsies which affects their treatment process and thus theirs overall health. Research findings manifest that a five-year survival rate (≈ 45%) after all the medication has not upgraded over the past few decades. The major causes of the poor survivability are delay in diagnosis and lack of early symptoms [1-5]. As a consequence, there is need of portable devices which to be sensitive, rapid in detection, cheaper, and easily operated. Along with it, AI tools coupled with fluorescence device are also required for real time motoring.

To achieve the non-invasive detection, optical devices namely fluorescence, Raman, OCT, life-time, diffuse reflectance etc. are utilized by the researchers [6-13]. In the optical systems/devices, steady-state fluorescence-based spectroscopic devices are reasonably deployed for in-vivo detection of oral cavity lesions [14-26]. Principle of fluorescence devices are based on light tissue interaction. A biological tissue contains endogenous fluorophores named as Tryptophan, Collagen, NADH, FAD, porphyrin etc. These fluorophores yield fluorescence light when irradiated by a particular wavelength (λ) of light. The excitation wavelength of Tryptophan, Collagen, NADH, FAD, and Porphyrin molecules are nearby 280, 325, 340, 450 and 400 nm and their emission bands lie near the visible region i.e. at 340, 390, 440, 530 and 635 nm respectively [16, 17]. It is accepted that fluorophore

*[1]Faculty of Engineering and Technology (FEAT), Datta Meghe Institute of Higher Education and Research (DMIHER), Wardha 442001, India. [2]Centre for Quantum Science and Technology, Sikha 'O' Anusandhan (SOA), Jagamara, Bhubaneswar, India. [3]Department of Applied Physics, Yeshwantrao Chavan College of Engineering (YCCE), Nagpur, India. [4]Sikha 'O' Anusandhan (SOA), Jagamara, Bhubaneswar, India. [5]Department of CSE, Yeshwantrao Chavan College of Engineering (YCCE), Nagpur, India. *For Correspondence: pavank.feat@dmiher.edu.inAcienden ditiorit rem et fuga. Et volupta quidis non eatent omnis sinctec taectes*

concentration alters with the development of lesions (benign → precancerous → OSCC) and these variations could be observed in the fluorescence spectra. Data analysis is also an important section for such clinical studies to predict/identify the various stages of cancer. For it, researches have used various statistical methods/tools. Some of the widely used tools for oral cancer identification are PCA, LDA, ANN, ROC, KNN, and SVM respectively [17-23].

In this paragraph, the key findings of the oral cancer research using the spectroscopic devices are briefly described. In this regard, Gillenwater et al. evaluated the potential of fluorescence spectroscopy on 15 patients (premalignant and malignant) and 8 healthy volunteers and attained a sensitivity of 88.2% and a specificity of 100% by the use of diagnostic algorithm [15]. Inaguma M and Hashimoto K examined 78 oral carcinomas patients using the fluorescence system and obtained the porphyrin-like fluorescence in 66 patients (85%) whereas the normal region did not exhibit. [16]. Van Staveren HJ et al. [17] group in an in-vivo study by the fluorescence spectroscopy system on 21 oral leukoplakia patients and 2 normal oral mucosa (six locations) concluded that leukoplakia could be distinguished to normal with sensitivity 86% and specificity of 100% by ANN. Diana C.G. de Veld et al. group executed a comprehensive study for in-vivo detection of oral lesions. In their first work, they conducted measurements on oral tissues of healthy volunteers (control group) only and reported the differences in the fluorescence intensities values among the sites of oral cavity [18]. In other work, they performed measurements on three groups i.e., benign, dysplastic (premalignant), malignant lesions at λexc = 350-450 nm and recorded the fluorescence spectra. They demarcated the malignant lesions from control (healthy) with ROC-AUC score of 0.97 [19]. Majumder et al. group also contributed with the development of a laser inducted fluorescence-based system (λ = 337 nm) and reported that nonlinear MRDF exhibited greater performance (sensitivity = 95%) than the linear PCA based algorithm (sensitivity = 80%) in distinguishing cancerous tissue from the normal [20]. By the make use of spectroscopic systems for the monitoring of oral lesions, Jayanthi et al. group attain AUC-ROC score of 0.98 for auto-fluorescence (AF) and 0.99 for diffuse reflectance (DR) respectively [21]. A fluorescence-based handheld device utilized by the Lane et al. group for the visualization of oral cavity lesions, segregated the lesions with the sensitivity of 98% and specificity of 100% [22]. Flugge et al. group detected OSCC lesions on clinical photograph and achieved accuracy of 0.98 by the deep learning approach [23]. Our group also conducted a clinical study for the detection of oral cancer using a fluorescence based portable device. Statistical methods such as PCA, SVM, ROC, and Mahalanobis distance models employed for classification had manifested excellent results [24 -26]. Nayyar et al. group did the screening of OSCC and OPMDs cases by fluorescence spectroscopy and imaging portable setup and noticed the red shift in cancerous tissue than normal [27]. Ramani S et al. group utilized confocal microscopy for in vivo assessment of oral lesions. They reported AUC values from 0.90 to 0.96 for distinguishing oral epithelial dysplasia, OSCC, lichenoid lesions and no dysplasia [28].

Here, we have presented a clinical study for in-vivo diagnosis of oral cavity lesions by a portable fluorescence probe as well as classification of all three groups by the AI tools. In-house build device, utilized for oral cancer detection displayed FAD band at λemi ≈ 500 nm and porphyrin bands at λemi ≈ 634, 676, 689, 703 nm in patients and volunteers. Intensity of porphyrin fluorescence is found larger in OSCC and dysplastic patients. To discriminate among the three groups, AI tools namely PCA, Naïve Bayes, KNN, LDA, and QDA were implemented in which PCA based QDA tool had shown slightly better classification than the other tools.

Materials and Methods

Measurement technique

For in-vivo examination of oral cancer patients, we had made use of portable device based on the fluorescence. The working of the device is illustrated by a schematic ray diagram as pictured in Figure 1(a). It can be seen that the light coming from laser source (Model: ADR-1805, Pegasus Shanghai Optical System) incidents on the beam splitter (BS) through a collimating lens (UV-Visible) and

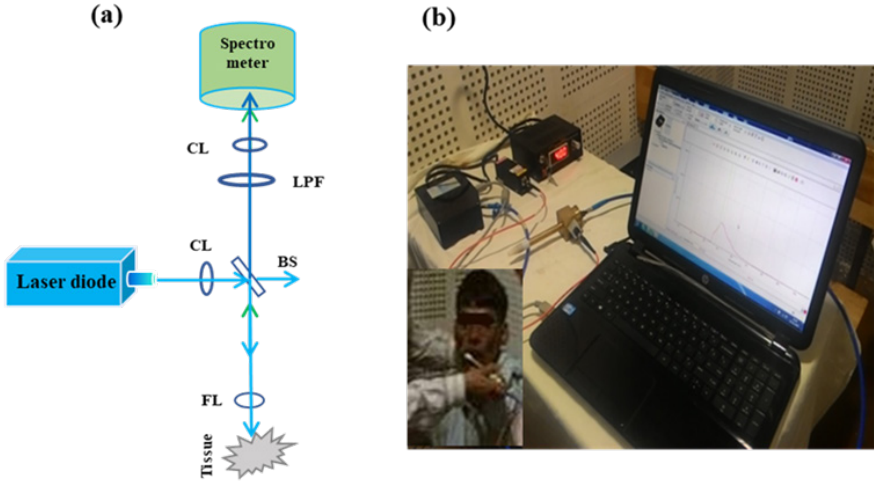

Figure 1. (a) Ray diagram (b) Image of the device with all accessories required to execute measurements

breaks into two components. One of the components, goes in the same direction and another at right angle i.e., toward the sample via a focusing lens. It can be seen in the Figure 1b that a cap made of Teflon material is placed at lower side of probe. It is positioned in such a fashion that focused light could touch the end of tip and to be at center so that maximal fluorescence light could be attained. Fluorescence signal generated by the fluorophores are recorded by the spectrometer. A long pass filter (LPF) kept in the rear side of the spectrometer eliminates the specular reflection.

After the calibration of the device in lab, we installed it in the Hallet Hospital Kanpur, UP, India to evaluate its clinical potential. A photograph of the device with all the requisite such as laser, laptop etc. is illustrated in Figure 1(b). While acquiring the spectrum from each patient and volunteers, laser light (λexc = 405 nm) of an optimal power (≈ 122 μW) was illuminated on the LBT site of oral cavity lesions and fluorescence signal were recorded by a highly sensitive UV-Visible spectrometer. At the time of measurement, light of the room was turned off. A 450 LPF (Model: FEL0450, Thorlabs, NJ, USA) was used to remove the specular reflection. An integration time of 3s was opted which was sufficient to achieve the fluorescence light from all the oral cavity tissue sites. Spectra-suit software was used to visualize the spectra and the interfacing between the spectrometer and laptop was done using a USB cable. After the completion of the measurements from a patient, cap was disposed.

Data collection

Fluorescence data was acquired from 55 LBT sites of 20 OSCC patients, 49 LBT sites of 18 dysplastic patients, and of 60 LBT sites of 36 clinically healthy volunteers (control) by the device. The mean age with the standard deviation was 47 ± 12 for OSCC, 39 ± 8 for dysplastic, and 36 ± 7 normal respectively. During the in-vivo measurements on patients, we had taken care the few points which are as follows. (i) A brief idea about the device and its advantages over the biopsy was expounded. (ii) Patients were instructed in advance not to consume stuff like food on the day of clinical examination. (iii) Advised to clean their oral cavity (iv) A consent form was taken to all the patients and volunteers. (vi) Their history like age, family background, life style, and frequency of consuming un-healthy products were noted in a questionnaire form. Afterwards patients were referred for biopsy.

Analysis methods (PCA, Naive Bayes, KNN, LDA, and QDA)

To analyze the spectroscopic data, we operated basic AI tools (supervised and unsupervised) such as principal component analysis (PCA), Naïve Bayes classifier, K-nearest neighbors (KNN) algorithm, linear and Quadratic discriminant analysis (LDA & QDA) respectively [29-34]. The objective of implementing PCA on the data set i.e., on spectral data was to lowering the dimension without losing the necessary information. It could be obtained by computing the eigen vectors also named as principal components. In it, the first five eigen values captures the total variance of ≥ 96%. PC scores corresponding to these five eigen values were computed and loaded in all the tools. A brief description about the AI tools is described here. Naïve Bayes are utilized to classify among the groups and this algorithm is built on the foundation of Bayes' theorem. By operating Bayes' theorem, Naive Bayes finds the probability of a given data point corresponds to a specific group/class and it is based on the feature values present in the data. KNN algorithm differentiate the groups by identifying the K nearest neighbors to a given data point and then by computing the distance (a simple distance calculation between the points known as Euclidean distance). The labelling of the classes is governed by the average of K neighbors. In LDA classification, it is assumed that the data for each class have Gaussian (normal) distribution and the identical correlation matrix (common correlation matrix). LDA finds the best linear decision boundary. However, in QDA, it is assumed that data is normally distributed but the correlation matrix for each class is not equal. The applicability of QDA is best when the classes have distinct variance or the decision boundary is not linear.

Results

Averaged spectra of all the three groups at λexc = 405 nm are shown in the Figure 3(a). Florescence Spectra are recoded from the lateral boarder of tongue (LBT) of the oral cavity in the spectral range of 450 to 750 nm. Averaged spectra consist of 55 tissue sites of 20 OSCC patient, 49 tissue sites of 18 dysplastic patient, and 60 tissue sites of 36 control group. In the spectra, presence of FAD and porphyrin bands at 500 nm and at 634, 676, 689, and 703 nm can be seen. Peak intensity values of porphyrin bands (634 nm) with the SD values for OSCC, dysplastic, and normal groups are 5450 ± 4510, 1650 ± 1300 and 447 ± 187 respectively. These peak intensity values with SD signify that there is significant difference in the fluorescence intensity values among the three groups as well as there is large variation in intensity values within the groups of OSCC and dysplastic groups. It can be seen that the difference in the peak values is significant. It can also be seen in the Figure 2(a) that intensity of porphyrin band in OSCC patients is slightly prominent than that of FAD band. In the dysplastic patients, it is lesser than the porphyrin band intensity. However, in healthy volunteers, intensity of porphyrin band is insignificant. A typical spectrum depicted in Figure 2(b), show that FAD band is prevailing in OSCC patient than the porphyrin band. However, in dysplastic patient, porphyrin band intensity is slightly greater than the FAD band intensity. It indicates that, it is not always true that intensity values of porphyrin will dominate over the FAD bands in all the cases and vice versa. This information describes that selection of entire spectral range is a good choice for the data analysis instead of choosing a specific biomarker.

Discussion

The increment in the fluorescence intensities of porphyrin bands with the advancement of oral mucosal

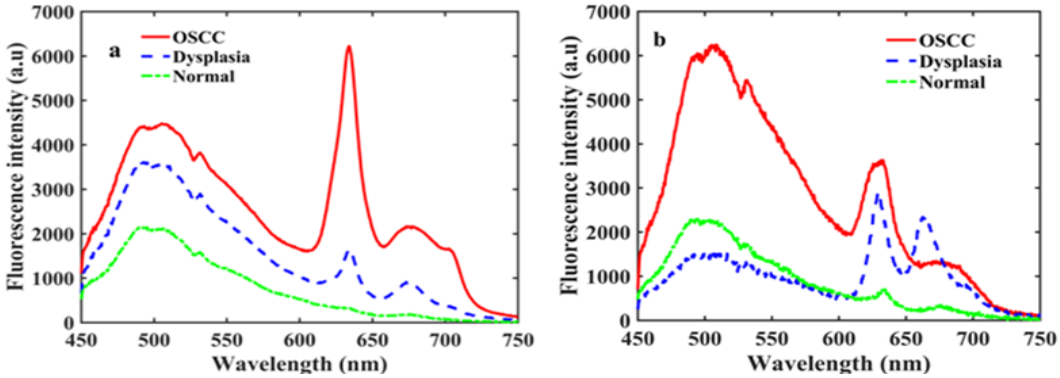

Figure 2. Spectra of OSCC, Dysplastic, and Normal Groups at Excitation Wavelength of 405 nm (a) averaged (b) typical

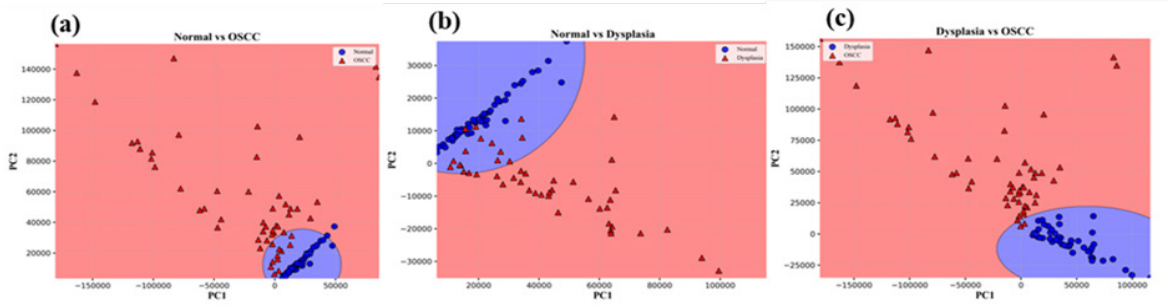

Figure 3. Naïve Bayes Boundaries Plots for (a) Normal to OSCC (b) Normal to Dysplasia (c) Dysplasia to OSCC

lesions indicates that concentration of porphyrin has risen, which was noticed in the recorded spectra. But the spectral pattern of both the OSCC and dysplastic patients have also shown that the higher intensities of porphyrin over the FAD bands was not found true for all the cases. Hence, analyzing the data by electing an individual biomarker would not be an appropriate procedure. However, investigating entire spectral data might be a better option. To distinguish the stages of oral lesions, the highest values of porphyrin and FAD bands from each group were picked and their ratios were estimated. ROC operated on the ratios (IPorphyrin/IFAD) were able to distinct

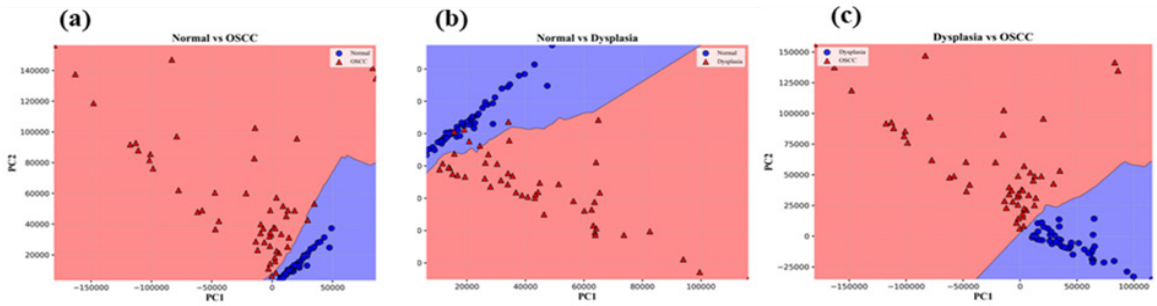

Figure 4. KNN Boundaries Plots for among the Three Groups

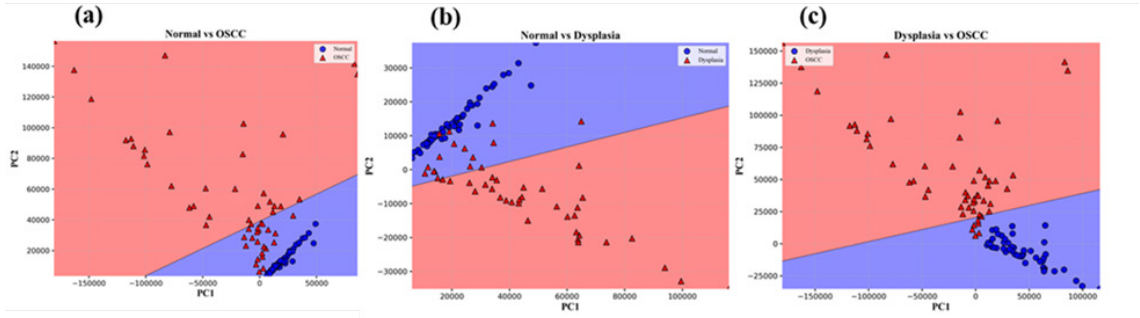

Figure 5. LDA Boundaries Plots for among the Three Groups

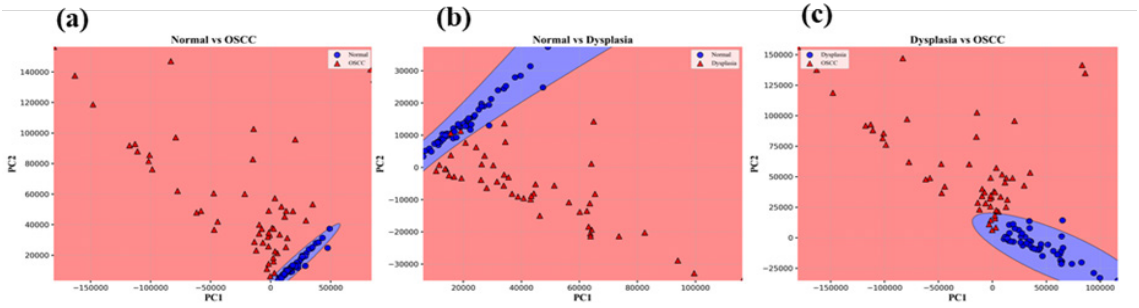

Figure 6. QDA Boundaries Plots for among the Three Groups

Table 1. Confusion Matrices for (I) Naïve Bayes (II) KNN (III) LDA (IV) QDA Data Sets

(I)	Naïve Bayes Confusion Matrix											
	Normal Vs. OSCC				Normal Vs. Dysplasia				Dysplasia Vs. OSCC			
	Training set		Testing set		Training set		Testing set		Training set		Testing set	
	41	1	17	1	42	1	17	0	33	1	14	1
	2	36	3	14	9	24	3	13	3	35	3	14
(II)	KNN Confusion Matrix											
	42	0	18	0	43	0	17	0	34	0	15	0
	2	36	2	15	0	33	5	11	0	38	0	17
(III)	LDA Confusion Matrix											
	42	0	18	0	43	0	17	0	34	0	15	0
	2	36	3	14	1	32	4	12	3	35	2	15
	QDA Confusion Matrix											
(IV)	42	0	17	1	33	1	15	0	43	0	17	0
	0	38	0	17	1	37	0	17	0	33	0	16

OSCC and Dysplasia from Normal with sensitivities and specificities of 98%, 83% and 100%, 98% respectively. However, OSCC from Dysplasia with sensitivity of 77% and specificity of 81%. Result shows that diagnostic parameters for the segregation of dysplastic to normal and OSCC to dysplastic groups are not good enough. It is therefore analyzing the data by the ratios of these two biomarkers is not a right choice. To enhance the diagnostic efficacy, we selected the entire fluorescence spectra. The recorded fluorescence data keeps the dimension of 700. The feature extraction was carried out by employing the PCA on the raw data. Eigen vectors correspond to first 5PC scores consist the variance of greater than 96%. However, first two PCs (PC1 & PC2) comprise of total 91% variance. It signifies that the useful information's are within the first few PCs. While applying the AI tools like Naïve Bayes, LDA, KNN, and QDA on the PC scores; segregation of PC scores into the two sets namely training and testing (validation) data sets were done. We took approximately 70% training data and 30% testing data and implemented various AI tools on these data. Scatter data plots obtained for these tools on first two PC scores are depicted in Figure 3, Figure 4, Figure 5 and Figure 6 respectively.

In the above scatter plots, one can notice the overlaps of the data points among the three groups. It reveals that investigating the data by including only first 2PC scores (PC1 & PC2) could not a correct approach. We therefore selected first 5 PC scores and employed all these AI tools one after the other. The confusion matrix for data sets (training & testing) of all the three classes acquired from Naïve Bayes, KNN, LDA, and QDA tools are tabulated in Table 1. In the Normal vs. OSCC group of Naïve Bayes training data, true negative (TN), false positive (FP), false negative (FN) and true positive (TP) are 41, 1, 2, 36 respectively. However, for testing data, the values of TN, FP, FN and TP are 17, 1, 3, and 14 respectively. Similarly for the other groups of AI tools, one can identify these values. By make use of these values, diagnostic parameters such as Sensitivity, Specificity, and overall accuracy between the groups can be estimated.

In test data (validation) of Normal vs. OSCC, we obtained sensitivities of 82.35%, 88.23%, 82.35%, 100% and overall accuracy values of 88.57%, 94.28%, 91.42%, 97.14% respectively by the Naïve Bayes, KNN, LDA and QDA respectively. In the testing data of Normal vs. Dysplasia, we obtained sensitivities of 81.25%, 68.75%, 75%, 100% with the overall accuracies of 90.90%, 84.84%, 87.87%, 100% respectively for the respective classifiers. However, in the testing data of Dysplasia vs. OSCC, sensitivities 82.35%, 100%, 88.23%, 100% and accuracies of 87.50%, 100%, 93.75% and 100% were achieved. Results demonstrate that QDA was able to discern with higher values of sensitivity.

A clinical study for oral lesions detection using the fluorescence device and the identification of various stages of lesions was executed. Among the fluorescence bands,

very weak porphyrin bands (634 nm only) were seen rarely in the spectra of control group. It was noticed that the intensity of 634 nm porphyrin band in several OSCC patients (≈ 85) was larger or equivalent to FAD band. On the other hand, it was more or less 30% in dysplastic patients. Classification accomplished by simple AI tools like Naïve Bayes, KNN, LDA, and QDA on the PC scores had shown fairly better accuracy for QDA. The overall accuracy values obtained by PCA based QDA tool was 97%, 100%, 100% respectively. The obtained results reveals that fluorescence-based device in conjunction with the PCA-based QDA tools could be an alternate to identification the stages of oral cavity lesions.

Author Contribution Statement

Dr. Pavan Kumar, who is the first author as well as corresponding author of this manuscript has worked on device development as well as on first draft of the manuscript. Apart from it, data collection and analysis were completed by the Dr. Kumar and Dr. Amar Nath Sah. Prof. Asima Pradhan and Dr. Vikrat worked on further refinement of manuscript.

Acknowledgements

The author (Dr. Pavan Kumar) is obliged to Dr. SK Kanaujia (ENT specialist) of GSVM Medical College Kanpur to collaborate with us on this project.

Approval

Corresponding author and other authors of this manuscript are agreed for publication.

Data Availability

Authors would be ready to provide data on request.

Study Registration

An approval from clinical trials registry India (CTRI) with registration number CTRI/2017/10/010102 was obtained.

Conflict of Interest:

Ethical Declaration

Ethical approval having the IEC communication number IITK/IEC/2015-16/2/10 was obtained to accomplish this clinical research study. It was first approved by internal committee members of IIT Kanpur and then by external members of GSVM Medical College, UP.

References

1. Ferlay J, Soerjomataram I. Dikshit R, Eser S, Mather C, Rebelo M et al (2015). Cancer incidence and mortality worldwide: sources, methods and major patterns in GLOBOCAN. https://doi.org/10.1002/ijc.29210.
2. Scully C, Bagan JV, Hopper C, Epstein JB (2008). Oral cancer: Current and future diagnostic techniques. Am J Dent, 21, 199-209. https://doi.org/10.1088/2516-1091/ac1f6c
3. Patton LL, Epstein JB, Kerr AR (2008). Adjunctive techniques for oral cancer examination and lesion diagnosis: a systematic review of the literature. J Am Dent Assoc, 139, 896–905. https://doi.org/10.14219/jada.archive.2008.0276.
4. Omar E (2015). Current concepts and future of noninvasive procedures for diagnosing oral squamous cell carcinoma-a systematic review. Head Face Med, 11, 1-27. https://doi.org/10.1186/s13005-015-0063-z.
5. Majumder SK, Keller MD, Boulos FI, Kelley MC, Mahadevan-Jansen A (2008). Comparison of autofluorescence, diffuse reflectance and Raman spectroscopy for breast tissue discrimination. J Biomed Opt, 13, 054009. https://doi.org/10.1002/lsm.20865.
6. DeCoro M, Wilder-Smith P (2010). Potential of optical coherence tomography for early diagnosis of oral malignancies. Expert Rev Anticancer Ther, 10, 321–29. https://doi.org/10.1586/era.09.191.
7. Alfano RR (2012). Advances in ultrafast time resolved fluorescence physics for cancer detection in optical biopsy. AIP Advances 2, 011103. https://doi.org /10.1063/1.3697961.
8. Ebenezar J, Aruna P, Ganesan S (2010). Synchronous fluorescence spectroscopy for the detection and characterization of cervical cancers in vitro. J Photochem Photobiol, 86, 77-86. https://doi.org/10.1111/j.1751-1097.2009.00628.x.
9. Tsai MT, Lee HC, Lee CK, Yu CH, Chen HM, Chiang CP et al (2008). Effective indicators for diagnosis of oral cancer using optical coherence tomography. Opt Exp, 16, 15847–62. https://doi.org/10.1364/oe.16.015847.
10. Singh SP, Deshmukh A, Chaturvedi P, Murali KC (2012). In vivo Raman spectroscopic identification of premalignant lesions in oral buccal mucosa. J Biomed Opt, 17, 105002. https://doi.org/10.1117/1.JBO.17.10.105002.
11. Kumar P, Singh A, Kanaujia SK, Pradhan A (2018). Human saliva for oral precancer detection: a comparison of fluorescence & stokes shift spectroscopy. J Fluoresc, 28, 419-26. https://doi.org/10.1007/s10895-017-2203-2.
12. Kumar P (2022). Detection of inaccessible head and neck lesions using human saliva and fluorescence spectroscopy. Lasers Med Sci, 37, 1821-1827. https://doi.org/10.1007/s10103-021-03437-4.
13. Onizawa K, Okamura N, Saginoya H, Yoshida H (2003). Characterization of auto fluorescence in oral squamous cell carcinoma. Oral Oncol, 39, 150–6. https://doi.org 10.1016/s1368-8375(02)00036-2.
14. Paderni C, Compilato D, Carinci F, Nardi G, Rodolico V, Muzio LL et al (2011). Direct visualization of oral-cavity tissue fluorescence as novel aid for early oral cancer diagnosis and potentially malignant disorders monitoring. Int J Immunopathol PharmacoL, 24, 121–128. https://doi.org /10.1177/03946320110240S221.
15. Gillenwater A, Jacob R, Ganeshappa R, Kemp B, El-Nagger AK, Palmer JL et al (1998). Noninvasive diagnosis of oral neoplastic based on fluorescence spectroscopy and native tissue autofluorescence. Arch Otolaryngol Head Neck Surg, 124, 1251-1258. . https://doi.org /10.1001/archotol.124.11.1251
16. Inaguma M, Hashimoto K (1999). Porphyrin-like fluorescence in oral cancer: in vivo fluorescence spectral characterization of lesions by use of a near-ultraviolet excited auto fluorescence diagnosis system and separation of fluorescent extracts by capillary electrophoresis. Cancer, 86, 2201-2211. https://doi.org/10.1002/(SICI)1097-0142(19991201)86:11<2201::AID-CNCR5>3.0.CO;2-9
17. Van Staveren HJ, Van Veen RL, Speelman OC, Witjes MJ, Star WM, Roodenburg JL et al (2007). Classification of clinical autofluorescence spectra of oral leukoplakia using an artificial neural network: A pilot study. Oral Oncol, 36, 286–93. https://doi.org/10.1016/s1368-8375(00)00004-x.

18. De Veld DC, Sterenborg HJ, Roodenburg JL, Witjes MJ (2004). Effect of individual characteristics on healthy oral mucosa autofluorescence spectra. Oral Oncol, 40, 815-823. https://doi.org/10.1016/j.oraloncology.2004.02.006.
19. De Veld DC, Witjes MJ, Sterenborg HJ, Roodenburg JL (2005). The status of in vivo autofluorescence spectroscopy and imaging for oral oncology. Oral Oncol, 41, 117-131. https://doi.org/10.1016/j.oraloncology.2004.07.007.
20. Majumder SK, Ghosh N, Kataria S, Gupta PK (2003). Nonlinear pattern recognition for laser-induced fluorescence diagnosis of cancer. Lasers Surg Med, 33, 48-56. https://doi.org/10.1002/lsm.10191
21. Jayanthi JL, Subhash N, Stephen M, Philip EK, Been VT (2011). Comparative evaluation of the diagnostic performance of autofluorescence and diffuse reflectance in oral cancer detection: a clinical study. Biophotonics, 4, 696-706. https://doi.org /10.1002/jbio.201100037.
22. Lane PM, Gilhuly T, Whitehead P, Zeng H, Poh CF, Samson NG et al (2006). Simple device for the direct visualization of oral-cavity tissue fluorescence," J. Biomed. Opt, 11, 024006. https://doi.org/10.1117/1.2193157.
23. Flügge T, Gaudin R, Sabatakakis A, Tröltzsch D, Heiland M, van Nistelrooij N, Vinayahalingam S (2003). Detection of oral squamous cell carcinoma in clinical photographs using a vision transformer. Sci Rep, 13, 2296. https://doi.org/10.1038/s41598-023-29204-9.
24. Kumar P, Kanaujia SK, Singh A, Pradhan A (2019). In vivo detection of oral precancer using a fluorescence-based, in-house-fabricated device: a Mahalanobis distance-based classification. Lasers Med Sci, 34, 1243-51. https://doi.org/10.1007/s10103-019-02720-9.
25. Sah AN, Kumar P, Pradhan A (2023). In vivo testing of oral mucosal lesions with in-house developed portable imaging device and comparison with the spectroscopy results. J of Flu, 26, 1-9. https://doi.org/10.1007/s10895-023-03152-z.
26. Kumar P, Rathod S, Pradhan A (2024). Detection of Oral Mucosal Lesions by Fluorescence Spectroscopy and Classification of Cancerous Stages by support vector machine," Lasers Med Sci, 39, 1-9. https://doi.org/10.1007/s10103-024-03995-3.
27. Nayyar V, Thapa P, Mehta DS, Yadav R, Bhatt K, Surya V el al (2024). Use of fluorescence imaging and spectrometry in detection of oral squamous cell carcinoma and oral potentially malignant disorders. Oral Oncol Rep, 9, 100172. https://doi.org/10.1016/j.oor.2024.100172
28. Ramani RS, Tan I, Bussau L, O'Reilly LA, Silke J, Angle C et al (2025). Convolutional neural networks for accurate real-time diagnosis of oral epithelial dysplasia and oral squamous cell carcinoma using high-resolution in vivo confocal microscopy. Sci Rep 15, 2555. https://doi.org/10.1038/s41598-025-86400-5.
29. Kumar P, Rathod S (2025). Integration of the fluorescence based portable device with the AI tools for the real-time monitoring of oral mucosal lesions. Sci Rep, 15, 10222. https://doi.org/10.1038/s41598-025-94676-w
30. Abdi H, Williams LJ (2010). Principal component analysis, Wiley Interdiscp Rev: Comput. Sta, 2(4), 433–459. https://doi.org/10.1002/wics.101
31. Alkhadar H, Macluskey M, White S, Ellis I, Gardner A (2021). Comparison of machine learning algorithm for the prediction of five-year survival in oral squamous cell carcinoma. J Oral Pathol Med, 50, 378-84. https://doi.org/10.1111/jop.13135.
32. Kumar P, Ganvir HV, Ganvir VY, Rathor S, Jamkar DV (2024). Classification of the Oral Mucosal Lesions Using the Principal Component Analysis Based Naïve Bayes Classifier: Fluorescence Spectroscopy as a Detection Device. ICETEMS, 513-517. https://doi.org/10.1109/IDICAIEI61867.2024.10842705
33. Kumar P, Pradhan A (2023). Human Saliva as a Substitute Diagnostic Medium for the Detection of Oral Lesions Using the Stokes Shift Spectroscopy: Discrimination among the Groups by Multivariate Analysis Methods. APJCP, 24, 3757-63. https://doi.org/10.31557/APJCP.2023.24.11.3757.
34. Won NJ, Bartling M, Macchia JL, Markevich S, Holthousen S, Jagota A, et al (2025). Deep learning–enabled fluorescence imaging for surgical guidance: in silico training for oral cancer depth quantification. J Biomed Opt 30, 13706-S13706. https://doi.org/10.1117/1.JBO.30.S1.S13706.